PHASE TRANSITIONS AND MULTICRITICAL POINTS IN THE MIXED SPIN-2 AND SPIN-7/2 ISING FERRIMAGNETIC SYSTEM WITH TWO CRYSTAL FIELD INTERACTIONS

Fathi Abubrig[1] and Mohamed Gneper[2]

[1]Department of Physics, Faculty of Science, Alasmarya University, Zliten, Libya
Email: dr.fathomar@gmail.com
[2]Department of Physics, Faculty of Science, Alasmarya University, Zliten, Libya
Email:Mohammad 8873@ gmail.com

ABSTRACT

The critical temperatures of the mixed spin-2 and spin-7/2 Ising ferrimagnetic system with two crystal-field interactions, D_A for spin-2 and D_B for spin-7/2, are investigated in the absence of an external magnetic field by using the mean-field theory based on Bogoliubov inequality for the free energy. The ground-state phase diagram is constructed.The phase diagrams of the critical temperatures are obtained in the temperature-anisotropy plane and the thermal variation of the sublattice magnetizations is investigated in detail. Besides the second-order phase transition lines, two types of the first-order lines; one ending at tricritical points and the other ending at isolated critical points, are found.

Keywords:Mixed spin system; Ising model; Sublattice magnetization; Critical points; Anisotropy.

1. INTRODUCTION

In the last three decades,mixed spin Ising ferrimagnetic systems have attracted much interest because of their critical behaviors and that they have less translational symmetry than their single-spin counterparts since they consist of two interpenetrating unequivalent sublattices. For this reason, theyhave been proposed as possible models to describe a certain type of molecular-based magnetic materials studied experimentally [1–4].These

materials include bimetallic molecular-based magnetic materials in which two kinds of magnetic atoms alternate regularly and exhibit ferrimagnetic properties. The bimetallic chain complex $MnNi(EDTA)^{-}6H_20$ is an example of an experimental mixed-spin system [5]. Moreover, the increasing interest in these systems is mainly related to their technological applications in the area of thermomagnetic recording [6,7].Therefore, the synthesis of new ferrimagnetic materials isan active field in material science.

One of the earliest, simplest and the most extensively systems to be studied were the mixed-spin Ising systems consisting of spin-1/2 and spin-S (S > 1/2) in a uniaxial crystal field. In these systems,different approaches have been used: mean-field approximation [8], effective-field theory with correlations [9-15], cluster variational theory [16], renormalization-group technique [17] and Monte-Carlo simulation [18-26]. Mixed-spin Ising systems consisting of higher spins are not without interest. Indeed, several theoretical studies of mixed spin-1 and spin-3/2 Ising models based on different approaches have been reported: the effective-field theory, on the simple cubic, honeycomb and square lattices [27-29], mean-field theory based on the Bogoliubov inequality for Gibbs free energy [30**]**and by means of recursion relations on the Bethe lattice [31], and Monte Carlo simulation [32].

Recently, The attention was devoted to the high order mixed spin ferrimagnetic systems (mixed spin-3/2 and spin-2 ferrimagnetic system, mixed spin-2 and spin-5/2 ferrimagnetic system and mixed spin-3/2 and spin-5/2 system) in order to construct their phase diagrams in the temperature- anisotropy plane and to consider their magnetic properties. The

effect of a single-ion anisotropy on the phase diagrams of the mixed spin-3/2 and spin-2 Ising system by the use of the mean-field theory based on the Bogoliubov inequality for the free energy was investigated by Bobak and Dely [33]. They presented the phase diagrams and found that the system exhibit a tricritical point, triple point and an isolated critical point. Albayrak also used the exact recursion equations to study the mixed spin-3/2 and spin-2 Ising system with two different crystal-field interactions on Bethe lattice [34].The effective field theory was also used to investigate the magnetic properties of the ferrimagnetic mixed spin-3/2 and spin-2 Ising model under the effect of a longitudinal magnetic field on a honeycomb and a square lattice [35]. Fathi studied the mixed spin-2 and spin-3/2 [36] and the mixed spin-2 and spin-5/2 [37] Ising model with different crystal-fields for the two sublattices arranged alternatively by using the mean-field theory based on the Bogoliubov inequality for the free energy. He constructed the phase diagrams of these two systems and found interesting results. Finally, critical phenomena in mixed spin-3/2 and spin-5/2 Ising model on a square lattice was investigated by using Monte Carlo simulation[38].

The aim of this paper is to apply the mean-field theory based on Bogoliubov inequality for the free energy to construct the phase diagrams of the mixed spin-2 and spin-7/2 Ising ferrimagnetic system in order to investigate the effect of the crystal field interactions D_A of the sublattice A and D_B of the sublattice B on the critical points (second order, first order and tricritical temperatures) of this system, as well as the temperature dependences of the magnetizations in some particular cases.

The outline of this work is as follows. In Section 2, we define the model and its solution by using the mean-field theory based on the Bogoliubov inequality for the free energy. In section 3, the phase diagrams for various values of the single-ion anisotropies are discussed, as well as the temperature dependences of the magnetizations in some particular cases. Finally, Section 4 is devoted to the conclusions.

2. THE MODEL AND FORMULATION

The system we consider is a mixed Ising spin-2 and spin-7/2 ferrimagnetic system. This system is consisting of two sublattices *A* and *B*, which are arranged alternately. The Hamiltonian of this system can be written as:

$$\mathcal{H} = \mathcal{H}_{ij} = -J \sum_{i,j} S_i^A S_j^B - D_A \sum_{i=1}^{N/2} \left(S_i^A\right)^2 - D_B \sum_{j=1}^{N/2} \left(S_j^B\right)^2 \qquad (1)$$

where J (J< 0) is the nearest-neighbour exchange interaction. The sites of sublattice A are occupied by spins S_i^Ataking the values of ±2, ±1, 0 , and the sites of sublattice *B*are occupied by spins S_j^B and taking the values of ± 1/2, ± 3/2, ± 5/2, ± 7/2, D_A and$D_B$are the crystal–field interactions acting on the spin-2 and spin-7/2 respectively.The first summation is carried out only over nearest-neighbour pairs of spins on different sublattices.

The approximated free energy of this system is obtained from a variational method based on Bogoliubov inequality[39] and is given by the following inequality.

$$F(\mathcal{H}) \leq \Phi \equiv F_0(\mathcal{H}) + \langle \mathcal{H} - \mathcal{H}_0 \rangle_0, \qquad (2)$$

where $F(\mathcal{H})$ is the true free energy of the model described by the Hamiltonian given in (1).$F_0(\mathcal{H})$is the average free energy of a trial Hamiltonian $\mathcal{H}_0$ which depends on variational parameters. $\langle \mathcal{H} - \mathcal{H}_0 \rangle_0$denotes a thermal average of the value $\mathcal{H} - \mathcal{H}_0$over the ensemble defined by the trial Hamiltonian $\mathcal{H}_0$.

In this work, we use one of the simplest choices for this trial Hamiltonian which given by:

$$\mathcal{H}_0 = -\sum_i \left(\alpha_A S_i^A + D_A \left(S_i^A\right)^2\right) - \sum_j \left(\alpha_B S_j^B + D_B \left(S_j^B\right)^2\right), \qquad (3)$$

Where α_A is the variational parameter related to the spin S_i^A and $\alpha_B$is the variational parameter related to the spin S_j^B. By evaluating Eq. (2), it is easy to obtain the expression of the free energy per site in MFA, with respect to α_A and α_B,

$$f \equiv \frac{\emptyset}{N} \leq -\frac{1}{2\beta}\left(\ln\left(1+\exp(4\beta D_a)\left(2\cosh(2\beta\alpha_B)+2A\cosh(\beta\alpha_B)\right)\right) + \ln\left(\begin{array}{c} 2\exp\left(\frac{49\beta D_B}{4}\right)\cosh(3.5\,\beta\alpha_A) \\ +2\exp\left(\frac{25\beta D_B}{4}\right)\cosh(2.5\,\beta\alpha_A) \\ +2\exp\left(\frac{9\beta D_B}{4}\right)\cosh(1.5\,\beta\alpha_A) \\ 2\exp\left(\frac{\beta D_B}{4}\right)\cosh(0.5\,\beta\alpha_A)\end{array}\right)\right)$$

$$+\frac{1}{2}\left[-zJ\langle S_i^A\rangle_0\langle S_j^B\rangle_0 + \alpha_A\langle S_i^A\rangle_0 + \alpha_B\langle S_j^B\rangle_0\right] \qquad (4)$$

where N is the total number of sites per lattice, z is the number of nearest-neighbors for every site and $\beta = \frac{1}{k_B T}$.

The sublattice magnetization per site m_A is given by:

$$m_A = \frac{4\,s \quad (2\beta\,\alpha_B)+2As \quad (\beta\,\alpha_B)}{2c \quad (2\beta\,\alpha_B)+2Ac \quad (\beta\,\alpha_B)+E} \qquad (5)$$

The sublattice magnetization per site m_B is given by:

$$m_B = \frac{7\sinh\left(\frac{7}{2}\beta\,\alpha_A\right)+5B\sinh\left(\frac{5}{2}\beta\,\alpha_A\right)+3\,C\sinh\left(\frac{3}{2}\beta\,\alpha_A\right)+D\sinh\left(\frac{1}{2}\beta\alpha_A\right)}{2\left(\cosh\left(\frac{7}{2}\beta\,\alpha_A\right)+B\cosh\left(\frac{5}{2}\beta\,\alpha_A\right)+C\cosh\left(\frac{3}{2}\beta\,\alpha_A\right)+D\cosh\left(\frac{1}{2}\beta\alpha_A\right)\right)}, \qquad (6)$$

where,

$A=\exp(-3D_A/k_BT)$, $E=\exp(-4D_A/k_BT)$, $B=\exp(-6D_B/k_BT)$,

$C=\exp(-10D_B/k_BT)$, $D=\exp(-12D_B/k_BT)$.

By minimizing the free energy in Eq. (4) with respect toα_A and α_B, we determine the two variational parameters in the form

$$\alpha_A = zJm_B, \qquad \alpha_B = zJm_B. \qquad (7)$$

As the set of equations (5) –(7) have several solutions for m_A and m_B, the stable solution is the one which leads to the minimum free energy f given by equation (4). In the neighborhood of the second order phase transition points of the system m_A and m_B are very small. For this reason, the second-order transition points can be obtained by expanding equations (4) ⎯ (6) to obtain a Landau-like expansion

$$f = f_0 + am_A^2 + bm_A^4 + cm_A^6 + dm_A^8 + \cdots \qquad (8)$$

Here, the coefficients f_0, a, and b of the expansion are given by:

$$f_0 - \frac{1}{2\beta}\left(\ln\left(1+2\exp(4\beta D_A)\right) + \ln\left(\begin{matrix}2\exp\left(\frac{4\ \beta D_B}{4}\right)+2\exp\left(\frac{2\ \beta D_B}{4}\right)\\ +2\exp\left(\frac{9\beta D_B}{4}\right)+2\exp\left(\frac{\beta D_B}{4}\right)\end{matrix}\right)\right) \qquad (9)$$

$$a=\frac{\frac{49t^2(A+4)}{2+2A+E}+\frac{25Bt^2(A+4)}{2+2A+E}+\frac{9Ct^2(A+4)}{2+2A+E}+\frac{Dt^2(A+4)}{2+2A+E}}{2+2B+2C+2D} \quad (10)$$

$$\begin{aligned}b=\ & \frac{1}{2+2B+2C+2D}\Bigg(\Bigg(\frac{49}{6}\frac{1}{(2+2A+E)^3}\big(t^4\big(49A^3t^2+588A^2t^2-8A^3-2A^2E\\ & +AE^2+2352At^2-36A^2+20AE+16E^2+3136t^2-156A-32E-128\big)\big)\\ & +\frac{25}{6}\frac{1}{(2+2A+E)^3}\big(Bt^4\big(25A^3t^2+300A^2t^2-8A^3-2A^2E+AE^2\\ & +1200At^2-36A^2+20AE+16E^2+1600t^2-156A-32E-128\big)\big)\\ & +\frac{3}{2}\frac{1}{(2+2A+E)^3}\big(Ct^4\big(9A^3t^2+108A^2t^2-8A^3-2A^2E+AE^2+432At^2\\ & -36A^2+20AE+16E^2+576t^2-156A-32E-128\big)\big)\Bigg)\\ & +\frac{1}{6}\frac{1}{(2+2A+E)^3}\big(Dt^4\big(A^3t^2+12A^2t^2-8A^3-2A^2E+AE^2+48At^2-36A^2\\ & +20AE+16E^2+64t^2-156A-32E-128\big)\big)\\ & -\frac{1}{2}\frac{1}{(2+2A+E)(1+B+C+D)}\Bigg(t^2(A+4)(49+25B+9C\\ & +D)\Bigg(\frac{49t^4(A+4)^2}{(2+2A+E)^2}+\frac{25Bt^4(A+4)^2}{(2+2A+E)^2}+\frac{9Ct^4(A+4)^2}{(2+2A+E)^2}\\ & +\frac{Dt^4(A+4)^2}{(2+2A+E)^2}\Bigg)\Bigg)\Bigg)\end{aligned} \quad (11)$$

Where, $t=\beta zJ$

From equations (10) an (11), it is clear that the coefficients a and b are even functions in J. The sublattice magnetizations m_A and m_B are very small near

the phase transition from an ordered phase ($m_A \neq 0, m_B \neq 0$) to the disordered (paramagnetic) phase ($m_A = 0,\ m_B = 0$).

3. RESULTS AND DISCUSSIONS

3.1. Phase diagrams

At zero temperature. By comparing the ground-state energies, given in Hamiltonian given in eq. (1) of different phases,the ground-state phase diagram is constructed and is shown in Fig. 1.

As shown in this figure, we find eight ordered ferrimagnetic phases with different values of $\{m_A, m_B, q_A, q_B\}$. These ordered phases are

$$O_1 = \left\{-2, \frac{7}{2}, 4.\frac{4}{4}\right\}, O_2 = \left\{-1, \frac{7}{2}, 1.\frac{4}{4}\right\}, O_3 = \left\{-2, \frac{5}{2}, 4.\frac{2}{4}\right\}, O_4 = \left\{-1, \frac{5}{2}, 1, \frac{2}{4}\right\}, O_5 = \left\{-2, \frac{3}{2}, 4, \frac{9}{4}\right\}, O_6 = \left\{-1, \frac{3}{2}, 1, \frac{9}{4}\right\}, O_7 = \left\{-2, \frac{1}{2}, 4, \frac{1}{4}\right\}, O_8 = \left\{-1, \frac{1}{2}, 1, \frac{1}{4}\right\},$$

and four disordered phases:

$$D_1 = \left\{0,0,0.\frac{4}{4}\right\},\ D_2 = \left\{0,0,0.\frac{2}{4}\right\},\ D_3 = \left\{0,0,0.\frac{9}{4}\right\}, D_4 = \left\{0,0,0.\frac{1}{4}\right\}.$$

where the parameters q_A and q_B are defined by:

$$q_A = \langle (S_i^A)^2 \rangle,\ q_B = \langle (S_j^B)^2 \rangle,$$

It should be mentioned that the ground state phase diagram is important in classifying the different phase regions of the model for the phase diagrams at higher temperatures.

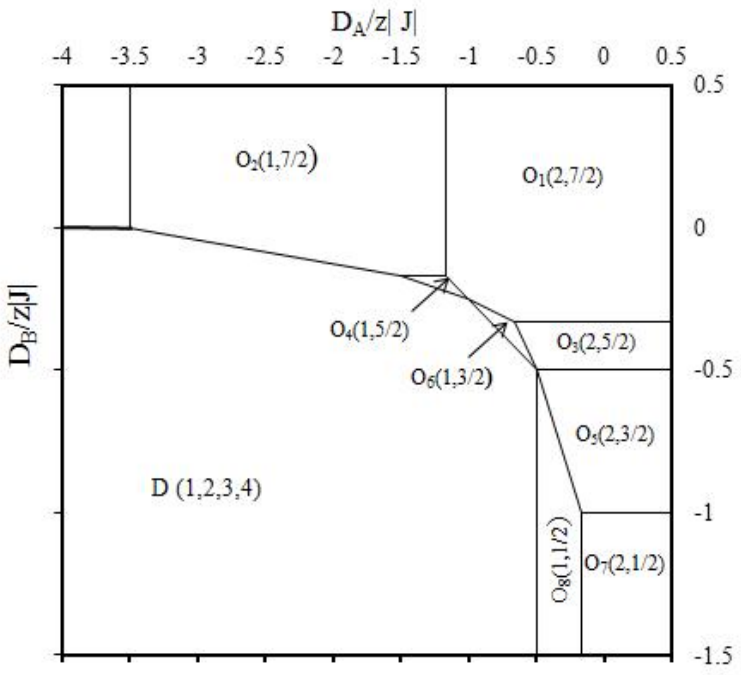

Fig..1. Ground-state p diagram of the mixed spin-2 and spin-7/2 Ising ferrimagnetic system with the coordination number z and different crystal-field interactions D_A and D_B. In this figure, we can see twelve phases. Eight ordered phases:($O_1, O_2, O_3, O_4, O_5, O_6, O_7, O_8$), separated by first-order transition lines and four disordered phases (D_1, D_2, D_3, D_4).

Now, by using the equations given in section 2, the phase diagrams of the system at finite temperature can be obtained in the (D_A, T) and (D_B, T) planes. The resulting phase diagram in the ($D_A/z|J|$, $k_BT/z|J|$) plane is shown in Fig. 2 for selected values of $D_B/z|J|$. In this figure, the solid and light dotted lines represents the second-order and first-order transition lines, respectively, while the heavy dashed curve represents the positions of tricritical points. These transition lines separate the ordered and the disordered phases when the temperature T > 0.

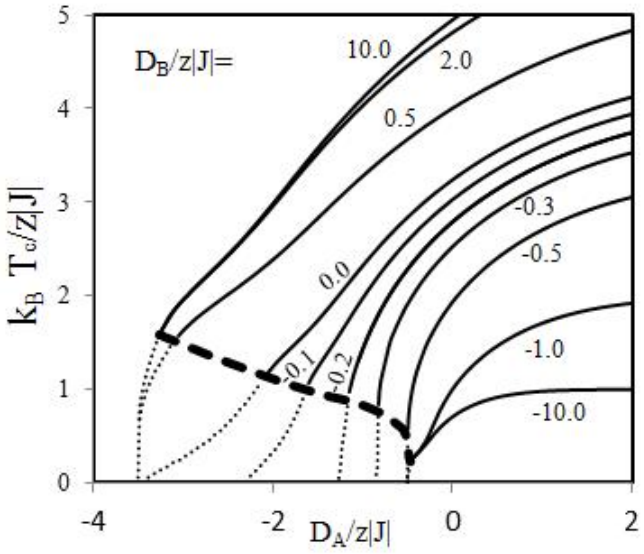

Fig. 2. Phase diagram in the (D_A; T) plane for the mixed-spin Ising ferrimagnet when the value of $D_B/z|J|$is changed. The solid and light dotted lines, respectively, indicate the second-and the first-order phase transitions, while the heavy dashed line represents the positions of the tricritical points.

It is easy to obtain the second-order phase transition lines from the two equations (10) and (11) under the conditions a=0 and b>0, while the tricritical points (the critical points at which the phase transitions change from second order to first order) are obtained from the same equations under the conditions a=0 and b=0, however, the first-order phase transitions must be determined by comparing the free energy, given in equation (4), of the ferrimagnetic phase (when the sublattice magnetizations m_A and m_B given by equations (5) and (6) are not equal to zero) with the free energy of the paramagnetic phase (when $m_A= m_B= 0$).

From figure (2), we note that there are two saturated tricritical points. The first point is in the limit of large positive D_B, when the spins behave like a

two-level system with $S_j^B = \square \frac{7}{2}$, and this point has the coordinates ($D_A/z|J|$, $k_BT_c/z|J|$)= (-3.2616, 1.5848), and the second point is in the limit of large negative D_B, when the system becomes equivalent to a mixed spin-2 and spin-$\frac{1}{2}$Ising model [8] and has the coordinates ($D_A/z|J|$,$k_BTc/z|J|$)=(-0.4659, 0.2264).For this reason, the coordinates of the first saturated tricritical point are seven times higher than the coordinates of the second tricritical point.

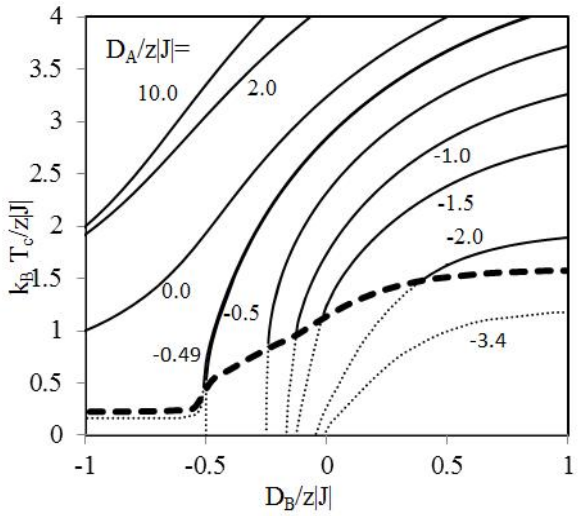

Fig. 3. Phase diagram in the (D_B ,T) plane for the mixed-spin Ising ferrimagnet when the value of $D_A/z|J|$is changed. The solid and light dotted lines, respectively, indicate the second- and the first-order phase transitions, while the heavy dashed line represents the positions of tricritical points.

In Figure 3, It is easy to note that the critical temperatures, which separate the ferrimagnetic phase from the paramagnetic phase, increase by increasing the crystal field interaction constants $D_A/z|J|$ and $D_B/z|J|$. This figure shows also that, for the region when the values of $D_A/z|J| > -0.4659$, this mixed-spin system includes second order phase transition lines only (solid lines),

for the region when $D_A/z|J| < -3.2616$, the system gives only first-order phase transitions and for the region when $-3.2616 < D_A/z|J| < -0.4659$, the system includes second order transition lines at higher temperatures, and first order transition lines (light dotted lines) at lower temperatures, separated by a curve of tricritical points (heavy dashed lines). This results can be compared with the results given in [30], [36], [37].

3.2. Sublattice magnetizations curves

In this subsection, The change of the sublattice magnetizations m_A and m_B with the temperature at different and selected values of the crystal field constants D_A and D_B, are obtained by solving the coupled equations (5) and (6) which are given in section. 2, numerically, and the results are depicted in Fig (4).

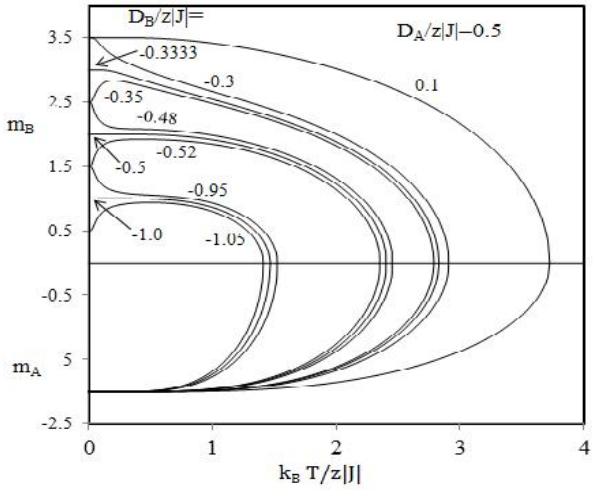

Fig. 4. The temperature dependences of the sublatticemagnetizations $m_A$andm_B for the mixed spin-2 andspin-7/2 Ising ferrimagnet with $D_A/z|J|=0.5$ when the value of $D_B/z|J|$ is changed.

Typical sublattice mag

0.5) and selected values of $D_B/z|J,|$ are shown in Fig. 4. Notice that the

values of $D_B/z|J|$ are selected to be located at the boundaries between the phases O_1,O_3,O_5 and O_7 or very close to them, in the ground state phase diagram given in Fig 1. As shown in Fig. 4, for $D_B/z|J| = 0.1$ (positive value which are located far enough from the boundary between the ordered phases O_1 and O_3), the sublattice magnetizationm_A and $m_B$show normal thermal variation behaviour (convex shapes).As $D_B/z|J|$ decreases from $D_B/z|J|= 0.1$ and approaches the boundaries between the O_1 phase and the O_3 phase, the O_3 phase and the O_5 phaseor the O_5 phase and the O_7 phase i.e, $D_B/z|J|=-0.3$, -0.48 or -0.95 (Note that these points are slightly higher than the boundaries).

.

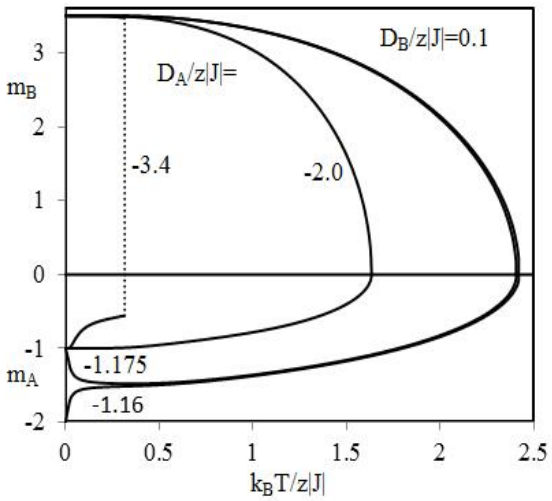

Fig. 5. The temperature dependences of the sublattice magnetizations m_A; m_B for the mixed spin-2 and spin-7/ 2 Ising ferrimagnet with $D_B/z|J| = 0.1$; when the value of $D_A/z|J|$ is changed.

In this case, the temperature dependence of m_B may exhibit a rather rapid decrease (damping) from its saturation value at T = 0K with the increase of

temperature and before m_B and m_A decrease to zero at the critical point. As shown in figure (4), when the values of $D_B/z|J$ = -0.3, -0.52,-1.05 which are slightly below the boundaries between O_1 and O_3, O_3 and O_5 or O_5,and O_7, respectively, the temperature dependence of m_B may exhibit initial-rise (excitation) of m_B with the increase of temperature before decreasing to zero at the critical point. It is clear from fig (4) that at the values of $D_B/z|J|$= -0.3333, -0.5, -1.0 (located on the boundaries between the mentioned phases O_1, O_3, O_5 and O_7 in the ground state phase diagram) the behaviours of the sublattice magnetization m_B, in this case, is similar to that given in Ref. [30], [36] and [37]. On the other hand, it is clear from figure (4) that for all values of $D_B/z|J|$ the sublattice magnetization m_A may show normal behaviour (convex shape) even though it is coupled to m_B.

The thermal variation of the sublattice magnetizations m_A and m_B are shown in Fig. 5 when the value of D_B is constant ($D_B/z|J|$=0.1) and with different values of $D_A/z|J|$. From this figure, it is clear that when the values of $D_A/z|J|$ = -1.175, -1.16 (very close to the boundary between the ordered phases O_1 and O_2 in the ground state phase diagram), the sublattice magnetization m_A may exhibit damping or excitation with the increase of temperature before decreasing to zero at the critical point, but m_B may exhibit a normal behaviour (convex shape). When the value of D_A= -3.4 (Located at the ordered phase O_1 and close to the boundary between this ordered phase and the disordered phase D_1) the sublattice magnetizations m_A and m_B may exhibit first order phase transition or jump from a certain value to zero at the first order critical point T_c.

3. 3. First order critical lines between the ordered phases

In figure.6.(a), the first orderboundaries between different ferrimagnetic phases at low temperatures are shown in small range in the (D_B, T) plane, when $D_A/z|J|$=-0.4995 (close to the point (-0.5,-0.5) at the ground state phase diagram). From this figure, it is clear that the curve which represents the boundaries between the distinct phases, in this case, can be divided into four different lines.The first line rises from an isolated critical point at a very low temperature and terminates at another isolated critical point (these isolated points are indicated by black circles) and separates the distinct ordered phases $O_5$and O_5'. The second line rises from the boundary between the ordered phases O_5 and O_8at T= 0K ,in the ground state phase diagram, and terminates at triple point T and this line separates the distinct phases O_5' and O_8'. The third line rises from triple point T and terminates at an isolated point and separates the distinct phases O_5' and O_6'. The fourth line rises from the same triple point and terminate at another isolated point and separates the distinct phasesO_6' and O_8'. In this figure, The second order phase transition line (solid line) and the first order phase transition line (dashed line), which separate the ferrimagnetic phase from the paramagnetic phase, are shown with the tricritical point (black square) that locates between these two lines.A closer view in the region of $D_B$is shown in figure.6 (b). In this figure, it is clear that there is a reentrant behaviour near the triple point. The triple point is the point which locates between three phases in the system.

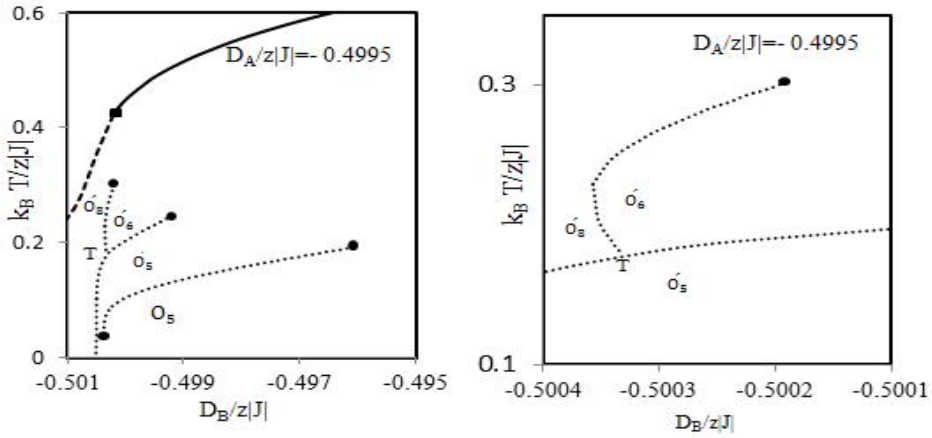

Fig. 6. (a) Low-temperature phase diagram in the (D_B; T) plane for the system when $D_A/z|J|$=-0.4995. The solid and dashed lines, respectively, indicate second and first-order transitions. O_5, O_5', O_6', a O_8' are distinct ordered ferrimagnetic phases The black circles correspond to the isolated critical points and T is a triple point. (b) A closer view in the region of D_B to show the reentrant behaviour near the triple point.

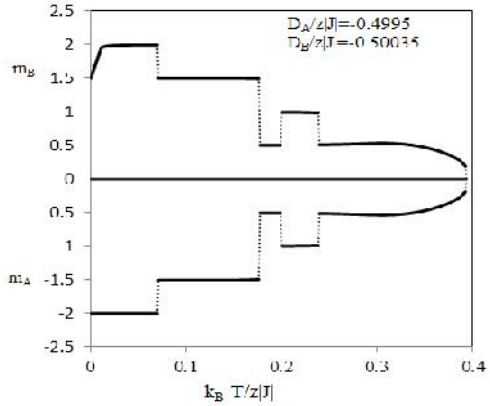

Fig. 7 The temperature dependence of the sublattice magnetizations m_A; m_B for the mixed-spin Ising ferrimagnet, when the value of $D_A/z|J$ =-0.4995 and the value of $D_B/z|J|$ = −0.50035, and refers to the phase diagram in Fig. 6 with four transition temperature points and one reentrance. The dotted lines indicate the first order transition and one reentrance.

In order to exc

region of the first order transition lines, separated the ordered phases, the sublattice magnetization curves which refer to the phase diagram given in

figure. 6 are depicted in figure. 7. In this figure, for the values of the selected crystal field constants$D_A/z|J|$=-0.4995 and $D_B/z|J|$=-0.50035, where five first transitions ($O_5 \rightarrow O_5' \rightarrow O_8' \rightarrow O_6' \rightarrow O_8' \rightarrow P$) occur. Thesublattice magnetization m_B exhibits rather rapid increase with the increase of temperature from T = 0K to a certain temperature T_1, while the magnetization m_B exhibits almost constant behaviour.

4. CONCLUSION

We investigated the phase properties and the magnetic behaviour of the mixed spin-2 and spin-7/2 Ising ferrimagnetic system in the framework of mean field theory. We have shown that the system undergoesfirst order critical transition lines and second order transition lines separated by tricritical line. In particular, we have obtained first-order critical lines separating different ordered phases at low temperatures and terminating at isolated critical points or triple point. We found that the system also displays a reentrant behavior close to the triple point location. Furthermore, at selected values of D_A and D_B, we have shown that when the temperature of the ferrimagnetic system increased from 0K to critical point, the sublattice magnetizations, m_A and m_B may exhibit four transition points that separate different ordered phases.

REFERENCES

[1] O. Khan, Molecular Magnetism, VCH Publishers, NewYork, 1993.
[2] T. Mallah, S. Thiebaut, M. Vardegauer, P. Veillet, Science. 262 (1993) 1554.
[3] H. Okawa, N. Matsumoto, H. Tamaki, M. Ohba, Mol. Cryst. Liq. Cryst. 233(1993) 257.
[4] C. Mathoniere, C.J. Nutall, S.G. Carling, P. Day, Inorg. Chem. 35 (1996) 1201.
[5] M. Drillon, E. Coronado, D. Beltran, R. Georges, J. Chem. Phys. 79 (1983) 449.
[6] J. Manriquez, G.T. Lee, R. Scott, A. Epstein, and J. Miller, Science. 252 (1991) 1415.

[7] W. Jiang, G.Z. Wei, and Z.Z. Zhang, Phys. Rev. 68 (2003) 134432.
[8] T. Kaneyoshi and J. C. Chen, J. Magn. Magn. Mater. 98 (1991). 201.
[9] T. Kaneyoshi, J. Phys. Soc. Japan. 56 (1987). 2675
[10] T. Kaneyoshi, Physica A. 153 (1988). 556
[11] T. Kaneyoshi, J. Magn. Magn. Mat. 92 (1990). 59
[12] A. Benyoussef, A. El Kenz, and T. Kaneyoshi, J. Magn. Magn. Mat. 131 (1994)173.
[13] A. Benyoussef, A. El Kenz, and T. Kaneyoshi, J. Magn. Magn. Mat. 131 (1994). 179.
[14] H. K. Mohamad, E. P. Domashevskaya, and A. F. Klinskikh, Physica A 388 (2009) 4713.
[15] A. Bobak, M. Jurcisin, Physica A. 240 (1997) 647.
[16] J.W. Tucker, J. Magn. Magn. Mater. 195 (1999) 733.
[17] S. G. A. Quadros and S. R. Salinas, Physica A. 206 (1994) 479.
[18] G. M. Zhang, C. Z. Yang, Phys. Rev. B. 48 (1993) 9452.
[19] G. M. Buendia, M. A. Novotny, J. Phys.: Condens. Matter. 9 (1997) 5951.
[20] G. M. Buendia, J. A. Liendo, J. Phys.: Condens. Matter 9 (1997) 5439.
[21] M. Godoy, W. Figueiredo, Phys. Rev. E 61 (2000) 218; 65 (2002) 026111, 66 (2002) 036131.
[22] G. Wei, Q. Zhang, and Y. Gu, J. Magn. Magn. Mater. 301 (2006) 245.
[23] G. Wei, Y. Gu, Jing Liu, Phys. Rev. B 74 (2006) 024422.
[24] M. Žukovič, A. Bobak, Physica A 389 (2010) 5401.
[25] M. Žukovič and A. Bobak, J. Magn. Magn. Mater. 322 (2010) 2868.
[26] R. A. Yessoufou, S. Bekhechi, F. Hontinfinde, Eur. Phys. J. B 81 (2011) 137.
[27] A. Bobak, Physica A 258 (1998) 140.
[28] A. Bobak, Physica A 286 (2000) 531.
[29] A. Bobak, O.F. Abubrig, D. Horvath, J. Magn. Magn. Mater. 246 (2002) 177.
[30] O.F. Abubrig, D. Horvath, A. Bobak, M. Jaščur, Physica A 296 (2001) 437.
[31] J.W. Tucker, J. Magn. Magn. Mater. 237 (2001) 215.
[32] Y. Nakamura, J.W. Tucker, IEEE Trans. Magn. 38 (2002) 2406.
[33] A. Bobak, J. Dely, J. Magn. Magn. Mater. 310 (2007). 1419.
[34] E. Albayrak . Physica A. **375** (2007) 174-184.
[35] B. Deviren, E. Kantar, E, M. Keskin, Journal of the Korean Physical Society, 56 (2010) 1738.
[36] F. Abubrig, Open Journal of Applied Sciences, 3 (2013) 218.
[37] F. Abubrig, Open Journal of Applied Sciences, 3 (2013) 270.
[38] N. De La Espriella Velez, J. Madera Yancez, M. S. Paez Mesa, Revista Mexicana de Fisica60(2014) 419.
[39] H. Falk, Am. J. Phys. 38 (1970) 858.